



<http://www.aimspress.com/>

---

### *Research article*

## **Pollution of soils and ecosystems by a permanent toxic organochlorine pesticide: chlordecone—numerical simulation of allophane nanoclay microstructure and calculation of its transport properties**

**Thierry Woignier<sup>1,2,\*</sup>, Florence Clostre<sup>3</sup>, Philippe Cattan<sup>4</sup> and Magalie Lesueur-Jannoyer<sup>3,5</sup>**

<sup>1</sup> Institut Méditerranéen de Biodiversité et d'Ecologie marine et continentale (IMBE), UMR CNRS 7263, Aix Marseille Université Avignon Université 13331, Marseille Cedex 03, France

<sup>2</sup> IRD UMR 237-Campus Agro Environnemental Caraïbes-B.P. 214 Petit Morne, 97232, Le Lamentin, Martinique

<sup>3</sup> Cirad/CAEC, UPR fonctionnement agroécologique et performances des systèmes de culture horticoles, B.P. 214 Petit Morne, Martinique, F-97285, Le Lamentin, France

<sup>4</sup> UPR Fonctionnement écologique et gestion durable des agrosystèmes bananiers et ananas, CIRAD, Capesterre-Belle-Eau, Guadeloupe, F-97130, France

<sup>5</sup> Cirad UR HortSys, TA B-103/PS4, Boulevard de la Lironde, F-34398 Montpellier Cedex 5, France

\* **Correspondence:** Email: [thierry.woignier@imbe.fr](mailto:thierry.woignier@imbe.fr); Tel: +596-596-42-30-34;  
Fax: +596-596-42-30-01.

### **Abstract:**

Pest control technology was introduced into the tropics without considering the specificity of their ecosystems and the risk of pollution was underestimated. Some volcanic soils (andosols) contain nanoclay (allophane) with a unique structure and porous properties compared to crystalline clays. Andosols are characterized by large pore volume and pore size distribution, a high specific surface area, and a fractal structure. These soils are more polluted than the other kinds of tropical soils but release less pollutants (chlordecone) to water and plants. The literature shows that the allophane microstructure favors accumulation and sequestration of chlordecone, an organochlorine pesticide, in andosols.

We used a numerical model to simulate the structure of allophane aggregates. The algorithm is based on a cluster-cluster aggregation model. From the simulated data, we derived the structural features, pore volume and tortuosity, and its transport properties, hydraulic conductivity and diffusion. We show that transport properties decrease because of the presence of allophane. We

propose that low hydraulic conductivity and diffusion are important parameters to explain the high concentrations and trapping of pollutants in andosols.

**Keywords:** chlordecone; organochlorine pesticides; soil contamination; allophane clay; andosols; numerical simulation; hydraulic conductivity; diffusion

## 1. Introduction

The French West Indies are affected by severe agricultural pollution by chlordecone (CHLD). This organochlorine molecule persists in the soils of banana fields where it was applied more than 20 years ago [1,2,3], and until now, no treatment has been found to remediate the situation. CHLD contaminates and will continue to contaminate all environmental compartments and trophic chains (soil, water, crops, animals and thus foodstuffs) for many years to come [1,4,5,6,7,8]. CHLD has a strong bioaccumulation and bio-amplification potential for aquatic organisms [7]. This leads to the contamination of the entire food web [7].

The effects of CHLD pollution on human health are clear (increased risk of prostate cancer, [9]; disturbed cognitive development of young children, [10]) and have led to severe regulations in some sectors including on the sale of agricultural and seafood products and restricted use of water and soils. The local population is still exposed to CHLD through food [11] making pollution of the soil by CHLD public health concern. The major challenge involved in pollution management is reducing exposure to decrease the risk of health consequences.

CHLD contaminate plants. The level of soil pollution and the type of plant root system play a major role in CHLD contamination of crops. The ability of a crop to be contaminated greatly depends on CHLD content in the soil water solution (and hence on the ability of the soil to release the pollutant) as well as on the composition and physiology of the plant's roots [4]. To ensure food safety, food crops must comply with regulations concerning the maximum residue limit in the marketed products, which requires changes in cropping systems [12].

CHLD dispersion is complex. CHLD contamination of the soil can be assessed using the WISORCH model [1], which simulates well the soil CHLD content, taking into account the past pesticide application and CHLD leaching by rain, thus it could be one way to estimate soil CHLD content in banana fields. This could reduce the cost of the measurement of CHLD content in soils, as a lot of banana fields are concerned by this pollution. The model describes also the dynamic evolution of soil CHLD content, thus giving an idea of natural soil depollution. It accounts for different behaviors according to the soil type (andosol, nitisol, ferralsol). Concerning transfer, studies have shown that agricultural systems affect water and pesticide transfer [2,13]. At the plot scale, because of the high infiltration capacity of volcanic soils (andosols), pesticide losses via infiltration are higher than losses via surface runoff [14]. At the watershed scale, pollution of surface water results in two types of processes: a predominant continuous contamination process, which originates mainly from drainage of the subsurface aquifer that feeds the river; and an event-dominated process, linked to overland flow, runoff and suspended solid transport [15].

Because CHLD is no longer used in banana fields, the soil is now the main reservoir of the pollutant and hence the main source of pollution today for plants and water. Our purpose is to show to what extent the type of soil can affect its transfer towards water and plants, and to explore the processes involved. To this end, we use experimental results and a modeling approach.

The paper is divided into three parts. In the first part, we describe the main literature results obtained on the effect of the type of soil on pesticide retention and on the pesticide transfer to water resources and crops. We conclude that the physical properties of a peculiar clay (allophane) play a role in the retention and transfer process.

In the second part, we simulate the tortuous microstructure of the allophane aggregates by numerical simulation with a “cluster-cluster aggregation model”.

In the third part, based on the simulated microstructure, we calculate the physical properties of the allophane aggregates and show that the pore volume and the tortuosity increase with the allophane content while the hydraulic conductivity decreases with the allophane content. Moreover the diffusion is one order lower in allophane aggregate than without porous structure. These results could explain why these volcanic soils trap the pollutants.

## **2. Contamination of soil, water, and crops by chlordecone**

### *2.1. Influence of soil type on pesticide retention*

Basically, soil contamination results from the interaction between the pesticide molecule and the organic and mineral constituents of the soil. Different processes are involved: degradation and transformation processes that determine the amount of pesticide at a given time; processes that determine the distribution of pesticides between plants, air, water, and soil, i.e. plant uptake, volatilization, sorption/desorption processes on soil particles including the formation of bound residues; transport processes, notably related to the flow of water in the soil. All these processes depends on many factors: pH and temperature affect solubility; organic matter and the type of clay affect sorption and desorption processes; soil structure and the type of porosity affect water dynamics, notably pore size and pore distribution, and may create preferential flows [16,17]. Consequently, the fate of a pesticide will vary according to the prevailing conditions at the place it crosses in relation with variations in the physical, chemical, and biological conditions, either vertically, with depth in the soil profile, or horizontally, i.e. from one type of soil to another [18,19].

In the French West Indies (FWI) where CHLD was applied, pesticides interact with the three main types of soil cultivated in this area: andosol, nitisol and ferralsol (FAO soil classification). Across the world, different authors have shown that andosols have a higher sorption capacity for a range of pesticides than other soil types. Paton et al. [20], found that Dichlorophenol and Pentachlorophenol were tightly bound to the organic fractions within the andosols. In Mexico, in the case of two organophosphorus insecticides, parathion and cadusafos, the amounts of bound residues were higher in andosols than in vertisols (topsoil) [21]. Prado et al. [22] also demonstrated that andosols have a higher atrazine sorption capacity than vertisol with  $K_d$  values roughly one order of magnitude higher. Finally, in the French West Indies, sorption (partition coefficient) of cadusafos was also shown to be globally higher in andosol than in nitisol [23].

Similarly, concentrations of CHLD in andosols have always been shown to be higher than in ferralsols and nitisols (Table 1) whatever the study, and soil type has been shown to have an effect on plot contamination [1,2,3,24]. Likewise in the map of the risk of soil pollution by CHLD for Guadeloupe and Martinique fields, built on historical banana cropping duration and soil type, estimated contamination levels in andosol were globally higher than in other soils [25,26].

**Table 1. Mean CHLD content in soil ( $\text{mg}\cdot\text{kg}^{-1}$  dry soil, 0–30 cm) according to soil type, minimum and maximum CHLD contents and number of analyzed samples in parentheses when available [1,2,3,24].**

	Andosol	Ferralsol	Nitisol
Brunet et al. [24]	4.7 (0–19.8, $n = 169$ )	2.2 (0.1–6.2, $n = 55$ )	0.8 (0–2.3, $n = 12$ )
Cabidoche et al. [1]	10.8 (0.8–37.4, $n = 16$ )	2.3 (0.4–4.4, $n = 7$ )	0.7 (0.3–1.0, $n = 5$ )
Levillain et al. [2]	3.0	1.6	1.9
Clostre et al. [3]	9.5 (0.5–21.2, $n = 128$ )	2.4 (1.6–3.1, $n = 58$ )	/

Since CHLD has a low solubility, volatility and degradability, main attention was given to sorption/desorption process to explain differences from one soil to another. The soil-water partition coefficient relative to organic C content ( $K_{oc}$  in  $\text{m}^3 \text{kg}^{-1}$ ) partly accounts for this process. Cabidoche et al. [1] first proposed to assess  $K_{oc}$  in the three type of soil above, by inverting the WISORCH model that relates CHLD inputs and soil contamination. Results showed that andosol had a higher sorption capacity ( $K_{oc}$  of  $12\text{--}25 \text{ m}^3 \text{kg}^{-1}$ ) than ferralsol ( $K_{oc}$  of  $7.5\text{--}12 \text{ m}^3 \text{kg}^{-1}$ ) and nitisol ( $K_{oc}$  of  $2\text{--}3 \text{ m}^3 \text{kg}^{-1}$ ). Conversely, Fernandez Bayo et al. [23] were not able to statistically differentiate  $K_{oc}$  in an andosol from  $K_{oc}$  in a nitisol; in their study  $K_{oc}$  ranged from 1.2 to  $2.5 \text{ m}^3 \text{kg}^{-1}$  in all soils. But they reported higher sorption by andosols due to their higher organic content. In addition, they noted a very high desorption hysteresis (apparent hysteresis index,  $H < 0.43$ ), which may explain the difference of a factor of 10 between their results and those of Cabidoche et al. [1] for andosols. In fact, sorption study [23] used fresh input of CHLD. Conversely, in Cabidoche study [1], WISORCH model used measured values of CHLD content in water, i.e. resulting from desorption process since soil are currently the unique provider of CHLD. Consequently,  $K_{oc}$  were not calculated on the same bases: they resulted from sorption process in sorption study and desorption process in Cabidoche study. Finally, Fernandez-Bayo et al. [23], observed a higher affinity to soils with shorter alkyl chains, which they attributed to the characteristics of the organic matter. All of which is consistent with the fact that higher CHLD loads were observed in andosol than in other soils despite similar pesticide inputs [1,2]. However the literature shows that  $K_{oc}$  is a global concept behind which lie a series of explanations (hysteresis; organic matter content; composition of organic matter, etc.), which may make it possible to compare soils, but do not explain the origin of the differences.

## 2.2. Influence of soil type on water contamination

Water is the main vehicle of CHLD transport compare to air flow and soil erosion; so water flow is an important point to consider. Charlier et al. [27] observed that 76% to 90% of rainfall infiltrated and that shallow groundwater was the main contributor to the contamination of streams [15]. However, few studies have focused on pesticide transfers in andosols. In the case of CHLD, Cabidoche et al. [1] collected samples from lysimeters installed on an andosol and a nitisol. They observed that although CHLD concentration was only  $0.26 \text{ mg kg}^{-1}$  in the top nitisol (versus 4.6 in the andosol), the concentrations of CHLD in similar volumes of drainage water were 3 to 4 fold higher in the nitisol than in the andosol. This finding suggested that the desorption capacity of nitisol was higher than that of andosol. Finally, the global trend for andosol to better retain pesticides was confirmed by a leaching experiment (laboratory data), where transfer to percolating water was twice lower in the andosol than in the nitisol [28]. This reflects the complexity of the processes involved in the transport of pesticides in soil.

### 2.3. Influence of the soil type on crop contamination

Contaminated crops contain different concentrations of CHLD depending on the crop, organ, and type of soil. The most highly contaminated crops are roots and tubers followed by cucurbits and leaf vegetables. However, even if andosols are polluted at higher levels than non-allophanic soils (nitisols and ferralsols), crops grown on them are less contaminated than crops grown on nitisols and ferralsols [4,5,29] (Table 2). This contrasted soil behavior is a key to managing food safety and to promoting agricultural and food preparation practices that respect existing regulations and reduce the risk of exposure by the population [12].

**Table 2. Mean CHLD transfer from soil to crop ( $\text{mg}\cdot\text{kg}^{-1}$  dry weight in plant/ $\text{mg}\cdot\text{kg}^{-1}$  dry soil) according to the soil type (andosol or non-allophanic, i.e. nitisol and/or ferralsol).** In parentheses dispersion index (calculated as half the difference between the limits of the confidence interval) for [29] and [5] or standard deviation of the mean values for [4].

Crop	Harvested organ	CHLD transfer (CHLD plant/CHLD soil)	References
Yam (greenhouse)	Tuber		Cabidoche et Lesueur
<i>Non-allophanic</i>		0.0478 (0.018)	Jannoyer [4]
<i>Andosol</i>		0.0042 (0.0004)	
Yam (field)	Tuber		Clostre et al. [5]
<i>Non-allophanic</i>		0.116 (0.024)	
<i>Andosol</i>		0.032 (0.0065)	
Sweet potato (field)	Underground stem		Clostre et al. [5]
<i>Non-allophanic</i>		0.073 (0.015)	
<i>Andosol</i>		0.0365 (0.0065)	
Dasheen (field)	Corm		Clostre et al. [5]
<i>Non-allophanic</i>		0.552 (0.141)	
<i>Andosol</i>		0.0775 (0.016)	
Cucumber (field)	Fruit		Clostre et al. [29]
<i>Non-allophanic</i>		0.08 (0.007)	
<i>Andosol</i>		0.05 (0.01)	
Pumpkin (field)	Fruit		Clostre et al. [29]
<i>Non-allophanic</i>		0.07 (0.01)	
<i>Andosol</i>		0.08 (0.01)	

Observations of CHLD transfer from soil to plants led to the general assessment that andosol tends to retain CHLD more than other soils. Variables that account for sorption/desorption process of water transfer only make it possible to quantify the gap between andosol and other soils, but not to explore the physical or chemical processes that explain the differences. To advance in this respect, a structural hypothesis is proposed hereafter.

## 2.4. Influence of clay microstructure on pesticide trapping

It is widely admitted that the bioavailability of each pesticide is related to the physical-chemical properties of the pollutant, including its solubility in water, its chemical affinity with the soil organic matter, and biodegradability [30,31,32]. The structural properties of the mineral matrix with which pollutants are associated may also influence pollutant bioavailability and retention in soils [33,34,35,36]. In the literature [1], it is shown that andosols retain and trap more CHLD than other kinds of soils. A wide range of pesticides have been used for tropical volcanic soils and the general agreement is that the pesticides' sorption behavior is more pronounced in andosols. In the case of parathion, cadusafos, and 2,4-Dicchlorophenoxyacetic acid [21,37], the presence of the allophane clay in andosols greatly increased pesticide sorption. Allophane is made up of naturally occurring nanoparticles formed through the alteration of volcanic parent materials, and these particles are known to play a significant role in water retention, phosphorus storage and in the concentrations of heavy metals [38,39,40,41]. Allophanes are also known to be adsorbents for polluting chemical species [42] such as phosphates [43,44], arsenates [45,46], sulfates, molybdates, chromates and seleniates [46]. The AlOH and SiOH groups on the surface of the allophane give it interesting properties with respect to boron adsorption [42,44]. It is likely that the propensity of andosols for pesticide retention is related to the allophane microstructure and nanopore features. Data show that physical protection and adsorption of persistent pesticide are both higher in nano-sized structures [30,47,48]. The combination of pore size and network tortuosity may play a key role in controlling pesticide inaccessibility to microorganisms and water. The decrease in bioavailability has often been explained by slow diffusion in small pores and can be physically explained as the result of entrapment of molecules [49,50,51].

Some researchers describe allophane aggregates as “gel like” [52,53]. In its natural state, the clay consists of aggregations of spherical allophane particles [54,55,56]. Allophane spherules tend to form porous nano-sized aggregates [57,58], whose average diameter is around 100 nm, and there is a clear analogy between allophane aggregates and synthetic silica gels [44,54,59,60]. Allophane aggregates are amorphous alumino-silicate compounds with a fractal geometry [54,60,61]. Transmission electron microscopy shows allophane nano-spheres with a diameter of about 5 nm, the allophanic particles then aggregate and form clusters [54,57,61,62]. Small angle X-ray scattering (SAXS) showed the allophane aggregates to be fractal clusters with a fractal dimension close to 2.5–2.7 [62]. The tortuous structure of the allophane aggregates is typically in the mesopore range 5–100 nm. A fractal approach is useful to model soils [63,64] as a heterogeneous porous medium and its hydraulic characteristics. Numerical simulations showed that the calculated permeability is low in such a tortuous porosity [65,66].

In the following section, we calculate the tortuosity and transport properties (hydraulic conductivity and diffusion) in allophane aggregates by numerical simulation.

## 3. Numerical simulation of the microstructure of allophane aggregates

### 3.1. Cluster-cluster aggregation model

One description of allophanic soils [52,54] is that of a very open structure made up of coarser particles (crystalline minerals, vitric materials), with the gel-like allophane occupying the space between them. It is reasonable to assume that the ability of a soil to trap pesticide is related to the pore features and physical properties, like hydraulic conductivity and diffusion. Unfortunately it is

not possible to measure these properties at the scale of allophanic aggregates. Here, we present the textural properties of allophanic aggregates calculated by numerical simulation and we propose a correlation between the calculated porous features and the pesticide trapping mechanism. We use a numerical model to simulate the structure and physical properties of aggregates. The algorithm is based on the cluster-cluster aggregation model [67,68], from which we derive some physical properties: pore volume, specific surface area, tortuosity, hydraulic conductivity and diffusion.

In the literature, it has been explained that allophane aggregates are natural gels [52,53,54,59,61]. Compared to other aggregation models like ballistic model [69] and random sequential adsorption [70], the cluster-cluster aggregation model quite satisfactorily describes typical structures of porous systems obtained via particle aggregation, like the sol-gel process [67,68]. To build a porous microstructure, a set of  $N$  particles of size ( $a_0 = 1$ ) are randomly placed in a cubic box. These particles are allowed to undergo a Brownian diffusive motion, and irreversibly stick together with a probability  $p$  equal to 1 when they come into contact. Aggregates of particles are also able to diffuse and to stick to particles or to other aggregates. The procedure is repeated until all particles aggregate. To simulate the structure of allophanic soils, we used a method considering two different kinds of particle, with smaller particles representing the allophanic particles and larger particles representing the non-allophanic ones. Details of the method are described elsewhere [66].

### 3.2. Simulated textural properties

To calculate pore size distribution, we use a triangulation method in the pore space. The total pore space of the sample is measured by visiting the random points initially generated and placed in the void space of the sample. Details of the method are described elsewhere [71]. Measuring the frequency of the appearance of a particular pore diameter yields the pore size distribution. The mean pore size of the simulated structure ( $D_{sim}$ ) is extracted from the pore size distribution.

$$D_{sim} = \sum_i f_i D_i / \sum_i f_i \quad (1)$$

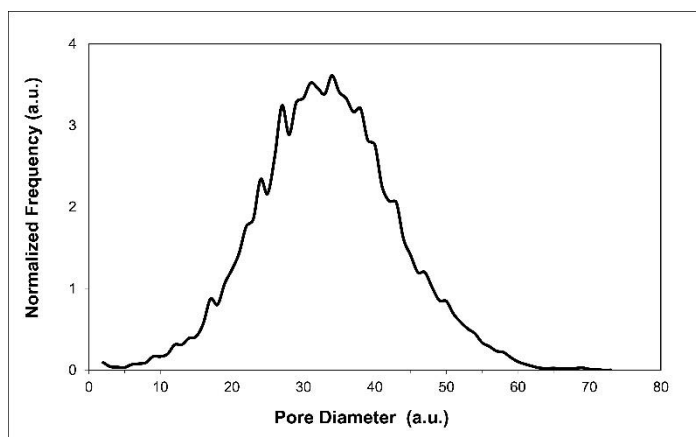
where  $f_i$  is the frequency of appearance of pore diameter  $D_i$ . The porous surface  $S_{sim}$  of the simulated porous systems is calculated as follows:

$$S_{sim} = \frac{\sum_{i=1}^N \sum_{j=1}^6 S_{ij}}{N} \quad (2)$$

where  $j$  denotes the nearest neighbors of an occupied site  $i$  (6 in a cubic lattice),  $S_{ij} = 1$  if site  $j$  is empty, and  $S_{ij} = 0$  if not. Thus,  $S_{sim}$  is the normalized number of free surfaces generated by the aggregation of the  $N$  particles. All numerical results reported in this work consist of a large average number of runs, never less than 50.  $D_{sim}$  and  $S_{sim}$  are dimensionless data (a.u.) because of the model particle size  $a_0 = 1$ .

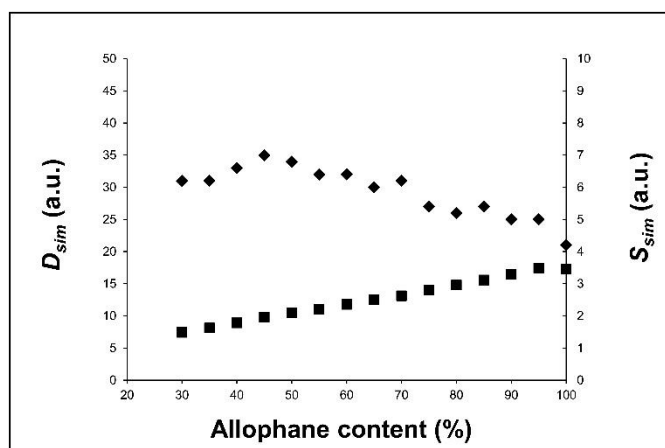
### 3.3. Simulation of the allophane aggregate porous properties

Figure 1 shows the typical pore size distribution curves obtained with the triangulation method.



**Figure 1. Typical pore size distribution curve (a.u.: arbitrary units).**

From the pore size distributions of the different allophane contents and relations 1 and 2, we calculated the evolution of the simulated mean pore size  $D_{sim}$  and porous surface  $S_{sim}$  versus allophane content (Figure 2). The pore size distribution and the derived porous features depend on allophane content of the soils. Allophane content is expressed in % of dry mass.



**Figure 2. Simulated mean pore  $D_{sim}$  (♦) and porous surface  $S_{sim}$  (■) versus allophane content.**

#### **4. Derivation of the physical properties of the allophane aggregates**

##### *4.1. Derivation of hydraulic diameter and specific surface area*

$D_{sim}$  and porous surface  $S_{sim}$  calculated by numerical simulation are dimensionless numbers and without physical meaning. However, it is possible to calculate the physical features like the hydraulic diameter ( $D_h$ ) and the specific surface area ( $S$ ) from the results of simulation with equations (3) and (4)

$$D_h = a D_{sim} \quad (3)$$

$$S = S_{sim}/(\rho_s a) \quad (4)$$



where  $a$  is the length of the allophane particle size,  $a = 3\text{--}5\text{ nm}$  [54] and  $\rho_s$  is the density of the solid matrix,  $\rho_s = 2.5$  [72].

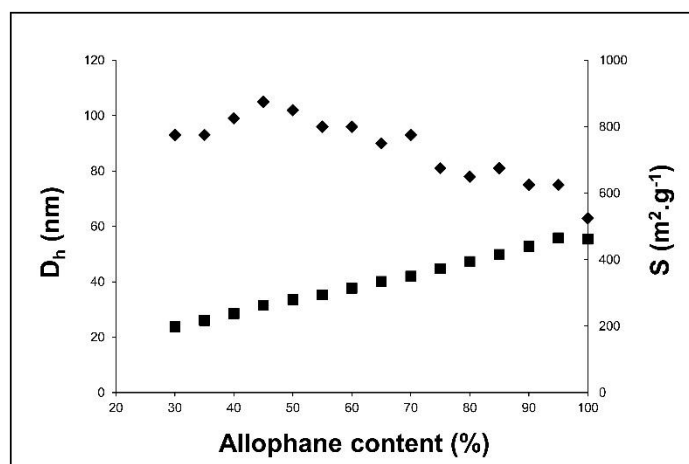


**Figure 3. Hydraulic diameter  $D_h$  (◆) and specific surface area  $S$  (■) versus allophane content.**

Figure 3 shows the hydraulic diameter and evolution of the specific surface area versus allophane content. The  $S$  evolution is more regular than  $D$  evolution because of the double sum ( $\Sigma$ ) which averages and smoothens the data.

The model is able to qualitatively account for the different experimental results on andosols, i.e. a decrease in  $D_h$  and an increase in  $S$  with an increase in allophane content [59,73].

#### 4.2 Derivation of the pore volume and hydraulic conductivity

Associated with the fractal (and consequently tortuous) structure, the hydraulic conductivity at the scale of the allophane aggregates will be low. Thanks to the simulated data, we can also calculate the pore volume (PV) and the hydraulic conductivity (HC) of the representative fractal aggregates [74]:

$$PV = D_{sim} S_{sim}/4 \rho_s \quad (5)$$

$$HC = \rho_s PV^3/5(PV \rho_s + 1) S^2 (\rho_w g/\mu) \quad (6)$$

where  $\rho_w$  is the density of water ( $\rho_w = 997.1\text{ kg}\cdot\text{m}^{-3}$ ),  $g$  is the gravitational acceleration ( $g = 9.81\text{ m}\cdot\text{s}^{-2}$ ) and  $\mu$  the dynamic viscosity ( $\mu = 0.89 \times 10^{-3}\text{ Pa}\cdot\text{s}$  at  $25\text{ }^\circ\text{C}$ ).

Figure 4 shows that HC is affected by allophane content and surprisingly decreases while pore volume increases. One could expect higher hydraulic conductivity with an increase in the pore volume, but the large increase in specific surface area has inversed the intuitive and expected tendency. The calculated HC correspond to permeability in the range of  $40\text{--}100\text{ nm}^2$ . This permeability range is in a good agreement with the permeability range of synthetic gels with a fractal structure [75].

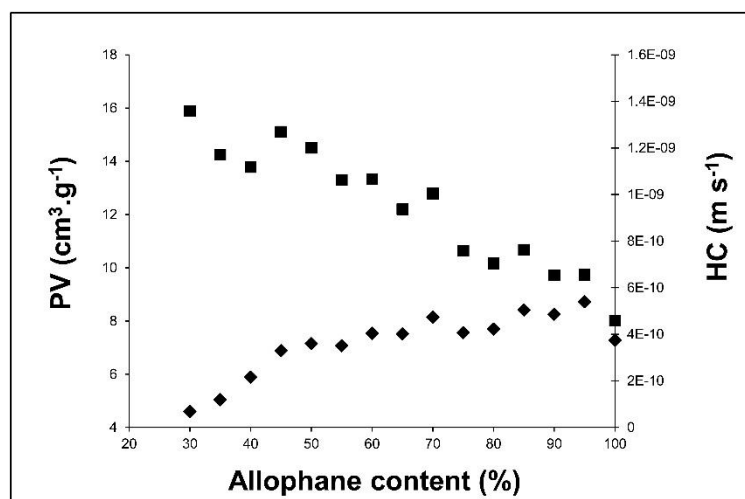


**Figure 4. Pore volume PV (♦) and hydraulic conductivity HC (■) versus allophane content.**

#### 4.3. Derivation of tortuosity and diffusion

Diffusion is an important transport process in geologic materials of low hydraulic conductivity. An understanding of the diffusion processes in the porous system is needed to be able to predict the fate and transport of contaminants. To this end, we must account for the tortuosity of the pore spaces. Diffusion along interstitial path with tortuosity  $t$  is reduced and gives:

$$D_i/D_{i0} = P/t^2 \quad (7)$$

where  $D_i$  is the diffusivity in the porous structure,  $D_{i0}$  is the diffusivity without porous structure ( $P = 1$ ),  $P$  is the porosity and  $t$  the tortuosity [76,77]. In a fractal aggregate, the tortuosity is also a power law function of the length scale:  $t \propto l^{\lambda-1}$  [69,78]. For silica gels, the exponent  $\lambda$  has been found experimentally to be between 1.4 and 1.8 [79,80], in quite good agreement with the predictions of aggregation models [81,82]. We have no  $\lambda$  value for the allophane aggregates, but we can assume that the  $\lambda$  value is not very different from the  $\lambda$  of silica gels successfully modelled with the cluster-cluster aggregation numerical approach [69].

The hydraulic diameter  $D_h$  is the typical length scale calculated for the “numerical allophane clay” and varies with the allophane content (Figure 2). From the  $D_h$  data, we calculate the tortuosity values as a function of the allophane content:

$$t_{(\text{allophane \%})}/t_{100\%} = D_{h(\text{allophane \%})}^{\lambda-1}/D_{h(100\%)}^{\lambda-1} \quad (8)$$

Tortuosity is difficult to measure [83]. In the absence of details concerning the tortuosity of the allophane aggregates and based on the allophane-gel analogy, we could assume that  $t_{100\%}$ , the tortuosity of the allophane aggregates with a 100% allophane concentration, is close to the tortuosity of silica gels. In the literature, the  $t$  value for silica gels has been reported to range between 1.5 and 2.4 [84,85,86,87]. Gas and liquid permeability leads to the conclusion that for composite gels,  $t$  is in the range 2–3. In the following, we use the value  $t_{100\%} = 2.5$ . From the relation (8) and using  $D_{h(100\%)} = 65$  nm (Figure 3), we calculated the evolution of  $t$  as a function of the allophane content. Figure 5 shows that the tortuosity varies between 2.4 and 3 with the allophane content.

Along with high tortuosity, we can calculate the associated  $D_i/D_{i0}$  evolution ( $t_0 = 1$  for  $P = 1$ ) (Figure 5). The diffusivity is one order of magnitude lower than  $D_{i0}$ . These results mean that water and chemical species will have difficulty diffusing inside the porosity of the fractal aggregates.

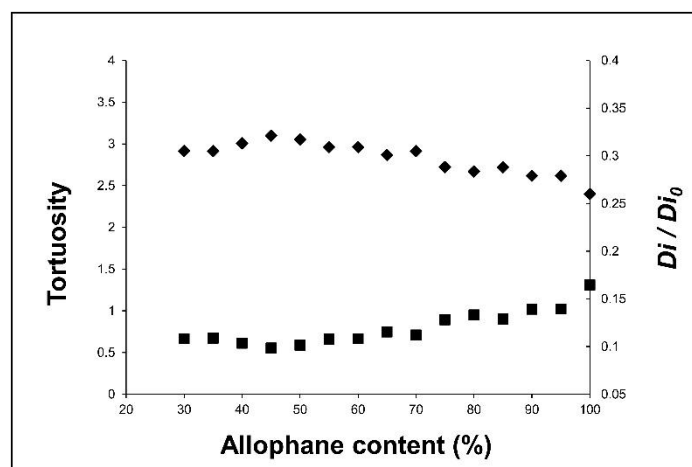


**Figure 5. Tortuosity (♦) and relative diffusion (■) versus allophane content.**

It is obvious that the real structure of the allophanic soils is much more complicated than the one built in this work with the cluster-cluster aggregation model. However, the goal of this approach is to give a simplified description of these peculiar soils in such a way to estimate physical properties that are not accessible using experimental techniques. The simplified description should account for the pertinent parameter related to the properties being studied. In this work, based on an analogy between gel structure and allophane aggregate, the significant parameter is the allophane content in the soils, which qualitatively controls the textural properties and all of the ensuing properties, like hydraulic conductivity and diffusion.

Using the numerical data, we have shown that HC and  $D_i$  are low in allophane aggregates. This way of numerically modelling the composite structure of allophanic soils and calculating physical properties could explain the higher pesticide sequestration in allophanic soils. In the tropics during the dry season, the andosols partially dry and because of capillary forces, the macropores empty while the micropores inside the allophane aggregates are full of water. Consequently, even if the diffusion process is hindered, the chlordecone slowly accumulates in the micropores of allophane aggregates. CHLD have a strong affinity with organic matter [1] and allophane aggregates contain large concentration of organic matter [64] which favors the binding of CHLD in the allophane. With such low hydraulic conductivity and diffusivity, the possible exchanges and chemical reactions with chemical species able to transform pesticides inside the aggregates are more difficult.

Finally, the pesticides stored in the vicinity or inside allophane aggregates will be difficult to extract. This conclusion is in qualitative agreement with results in the literature (see sections 1 and 2) showing that soils containing allophane store large amounts of pollutants.

## 5. Conclusion

Nanoparticles, with their large surface to volume ratio, appear to be a privileged site for the accumulation of pesticides. Andosols contain allophane, which presents unique structures and physical properties compared to crystalline clays. The features of allophane clay very closely

resemble those of porous materials synthesized by the sol gel process: large pore volume, broad pore size distribution, a high specific surface area, and a fractal structure. Fractal structure implies high tortuosity and thus a lower accessibility and availability of pollutant for diffusion processes.

With our numerical simulation, we have shown that, at the scale of the aggregates, the calculated transport properties are hindered by the allophane microstructure. These results could be important in explaining chlordecone sequestration in these soils. The tortuous and inaccessible microstructure of these nano-clays likely partly explains their exceptional capacity to immobilize and stock different kinds of chemical species and to trap pesticides.

This property represents a challenge for soil CHLD remediation: is it possible to use extraction processes? What about degradation by micro-organisms and their ability to reach the molecule? Fernandez-Bayo et al. [89] showed that 80% of CHLD remained extractable in an andosol. In addition, andosol structure (pore size distribution) may vary depending on soil preparation [88] or soil water contents (swelling). All of which suggest the trapping of CHLD may be reversible, even if the speed of release remains very low.

## Acknowledgments

Funding was provided by the French Chlordecone National Plan (“JAFA” project), the French National Research Agency (“Chlordexco” project, the French Ministry for Overseas development (MOM) and the France-Venezuela PCP program (“Matériaux Nanostructurés pour un développement durable” project).

## Conflict of Interest

All the authors declare no conflicts of interest in this paper.

## References

1. Cabidoche YM, Achard R, Cattan P, et al. (2009) Long-term pollution by chlordecone of tropical volcanic soils in the French West Indies: a simple leaching model accounts for current residue. *Environ Pollut* 157: 1697-1705.
2. Levillain J, Cattan P, Colin F, et al. (2012) Analysis of environmental and farming factors of soil contamination by a persistent organic pollutant, chlordecone, in a banana production area of French West Indies. *Agr Ecosyst Environ* 159: 123-132.
3. Clostre F, Lesueur-Jannoyer M, Achard R, et al. (2014) Decision support tool for soil sampling of heterogeneous pesticide (chlordecone) pollution. *Environ Sci Pollut Res* 21: 1980-1992.
4. Cabidoche YM, Lesueur-Jannoyer M (2012) Contamination of Harvested Organs in Root Crops Grown on Chlordecone-Polluted Soils. *Pedosphere* 22: 562-571.
5. Clostre F, Letourmy P, Lesueur-Jannoyer M (2015) Organochlorine (chlordecone) uptake by root vegetables. *Chemosphere* 118: 96-102.
6. Jondreville C, Lavigne A, Clostre F, et al. Contamination of grazing ducks by chlordecone in Martinique. Book of abstract; 2013; Nantes, France. Wageningen Academic Publishers. pp. 166-166.
7. Coat S, Monti D, Legendre P, et al. (2011) Organochlorine pollution in tropical rivers (Guadeloupe): role of ecological factors in food web bioaccumulation. *Environ Pollut* 159: 1692-1701.

8. Gourcy L, Baran N, Vittecoq B (2009) Improving the knowledge of pesticide and nitrate transfer processes using age-dating tools (CFC, SF<sub>6</sub>, 3H) in a volcanic island (Martinique, French West Indies). *J Contam Hydrol* 108: 107-117.
9. Multigner L, Ndong JR, Giusti A, et al. (2010) Chlordecone Exposure and Risk of Prostate Cancer. *J Clin Oncol* 28: 3457-3462.
10. Dallaire R, Muckle G, Rouget F, et al. (2012) Cognitive, visual, and motor development of 7-month-old Guadeloupean infants exposed to chlordecone. *Environ Res* 118: 79-85.
11. Dubuisson C, Héraud F, Leblanc J-C, et al. (2007) Impact of subsistence production on the management options to reduce the food exposure of the Martinican population to Chlordecone. *Regul Toxicol Pharm* 49: 5-16.
12. Lesueur-Jannoyer M, Cattan P, Monti D, et al. (2012) Chlordécone aux Antilles : évolution des systèmes de culture et leur incidence sur la dispersion de la pollution. *Agronomie Environnement & Sociétés* 2: 45-58.
13. Cattan P, Ruy SM, Cabidoche YM, et al. (2009) Effect on runoff of rainfall redistribution by the impluvium-shaped canopy of banana cultivated on an Andosol with a high infiltration rate. *J Hydrol* 368: 251-261.
14. Saison C, Cattan P, Louchart X, et al. (2008) Effect of Spatial Heterogeneities of Water Fluxes and Application Pattern on Cadusafos Fate on Banana-Cultivated Andosols. *J Agr Food Chem* 56: 11947-11955.
15. Charlier J-B, Cattan P, Voltz M, et al. (2009) Transport of a Nematicide in Surface and Groundwaters in a Tropical Volcanic Catchment All rights reserved. No part of this periodical may be reproduced or transmitted in any form or by any means, electronic or mechanical, including photocopying, recording, or any information storage and retrieval system, without permission in writing from the publisher. *J Environ Qual* 38: 1031-1041.
16. Clothier BE, Vogeler I, Magesan GN (2000) The breakdown of water repellency and solute transport through a hydrophobic soil. *J Hydrol* 231-232: 255-264.
17. Prado B, Duwig C, Etchevers J, et al. (2011) Nitrate fate in a Mexican Andosol: Is it affected by preferential flow? *Agr Water Manage* 98: 1441-1450.
18. Accinelli C, Vicari A, Pisa PR, et al. (2002) Losses of atrazine, metolachlor, prosulfuron and triasulfuron in subsurface drain water. I. Field results. *Agronomie* 22: 399-411.
19. Schiavon M, Perrin-Ganier C, Portal J (1995) La pollution de l'eau par les produits phytosanitaires : état et origine. *Agronomie* 15: 157-170.
20. Paton GI, Paterson CJ, Winton A, et al. (2004) Distribution, bioavailability and behavior of persistent organic pollutants in Andosols: with specific reference to Iceland. In: Arnalds HÓaÓ, editor. *Volcanic Soil Resources in Europe*. pp. 108-109.
21. Olvera-Velona A, Benoit P, Barriuso E, et al. (2008) Sorption and desorption of organophosphate pesticides, parathion and cadusafos, on tropical agricultural soils. *Agron Sust Dev* 28: 231-238.
22. Prado B, Duwig C, Hidalgo C, et al. (2014) Transport, sorption and degradation of atrazine in two clay soils from Mexico: Andosol and Vertisol. *Geoderma* 232-234: 628-639.
23. Fernandez Bayo J, Saison C, Geniez C, et al. (2013) Sorption characteristics of chlordecone and cadusafos in tropical agricultural soils. *Curr Org Chem* 17: 2976-2984.
24. Brunet D, Woignier T, Lesueur-Jannoyer M, et al. (2009) Determination of soil content in chlordecone (organochlorine pesticide) using near infrared reflectance spectroscopy (NIRS). *Environ Pollut* 157: 3120-3125.

25. Desprat J-F, Comte J-P, Chabrier C (2004) Cartographie du risque de pollution des sols de Martinique par les organochlorés : Rapport phase 3 : Synthèse. 25 p.
26. Tillieut O, Cabidoche Y-M (2006) Cartographie de la pollution des sols de Guadeloupe par la chlordécone : Rapport technique. Abymes, France: DAAF-SA & INRA-ASTRO. 23 p.
27. Charlier J-B, Cattani P, Moussa R, et al. (2008) Hydrological behaviour and modelling of a volcanic tropical cultivated catchment. *Hydrol Process* 22: 4355-4370.
28. Woignier T, Clostre F, Fernandes P, et al. (2015) Sequestering Pesticide with Organic Fertilizer or Organic Amendment. In: Shishir Sinha KKP, S. Bajpai, J.N. Govil, editor. *Fertilizer Technology*. USA: Studium Press LLC. pp. 319-344.
29. Clostre F, Letourmy P, Turpin B, et al. (2014) Soil Type and Growing Conditions Influence Uptake and Translocation of Organochlorine (Chlordecone) by Cucurbitaceae Species. *Water Air Soil Pollut* 225: 1-11.
30. Pignatello JJ (1998) Soil organic matter as a nanoporous sorbent of organic pollutants. *Adv Colloid Interfac* 76-77: 445-467.
31. Semple KT, Reid BJ, Fermor TR (2001) Impact of composting strategies on the treatment of soils contaminated with organic pollutants. *Environ Pollut* 112: 269-283.
32. Vlčková K, Hofman J (2012) A comparison of POPs bioaccumulation in *Eisenia fetida* in natural and artificial soils and the effects of aging. *Environ Pollut* 160: 49-56.
33. Peters R, Kelsey JW, White JC (2007) Differences in p,p'-DDE bioaccumulation from compost and soil by the plants *Cucurbita pepo* and *Cucurbita maxima* and the earthworms *Eisenia fetida* and *Lumbricus terrestris*. *Environ Pollut* 148: 539-545.
34. Chung N, Alexander M (2002) Effect of soil properties on bioavailability and extractability of phenanthrene and atrazine sequestered in soil. *Chemosphere* 48: 109-115.
35. Liu C, Li H, Teppen BJ, et al. (2009) Mechanisms Associated with the High Adsorption of Dibenzo-p-dioxin from Water by Smectite Clays. *Environ Sci Technol* 43: 2777-2783.
36. Rana K, Boyd SA, Teppen BJ, et al. (2009) Probing the microscopic hydrophobicity of smectite surfaces. A vibrational spectroscopic study of dibenzo-p-dioxin sorption to smectite. *Phys Chem Chem Phys* 11: 2976-2985.
37. Duwig C, Müller K, Vogeler I (2006) 2,4-D Movement in Allophanic Soils from Two Contrasting Climatic Regions. *Commun Soil Sci Plan* 37: 2841-2855.
38. Parfitt RL (1989) Phosphate reactions with natural allophane, ferrihydrite and goethite. *Journal of Soil Science* 40: 359-369.
39. Levard C, Doelsch E, Basile-Doelsch I, et al. (2012) Structure and distribution of allophanes, imogolite and proto-imogolite in volcanic soils. *Geoderma* 183-184: 100-108.
40. Doelsch E, Basile-Doelsch I, Rose J, et al. (2006) New Combination of EXAFS Spectroscopy and Density Fractionation for the Speciation of Chromium within an Andosol. *Environ Sci Technol* 40: 7602-7608.
41. Khan H, Matsue N, Henmi T (2006) Adsorption of Water on Nano-ball Allophane. *Clay Sci* 12: 261-266.
42. Reinert L, Ohashi F, Kehal M, et al. (2011) Characterization and boron adsorption of hydrothermally synthesised allophanes. *Appl Clay Sci* 54: 274-280.
43. Henmi T, Huang PM (1985) Removal of phosphorus by poorly ordered clays as influenced by heating and grinding. *Appl Clay Sci* 1: 133-144.
44. Clark CJ, McBride MB (1984) Cation and anion retention by natural and synthetic allophane and imogolite. *Clay Clay Miner* 32: 291-299.

45. Arai Y, Sparks DL, Davis JA (2005) Arsenate Adsorption Mechanisms at the Allophane–Water Interface. *Environ Sci Technol* 39: 2537-2544.
46. Opiso E, Sato T, Yoneda T (2009) Adsorption and co-precipitation behavior of arsenate, chromate, selenate and boric acid with synthetic allophane-like materials. *J Hazard Mater* 170: 79-86.
47. Calabi-Floody M, Velásquez G, Gianfreda L, et al. (2012) Improving bioavailability of phosphorous from cattle dung by using phosphatase immobilized on natural clay and nanoclay. *Chemosphere* 89: 648 - 655.
48. Baldock JA, Skjemstad JO (2000) Role of the soil matrix and minerals in protecting natural organic materials against biological attack. *Org Geochem* 31: 697-710.
49. Arias-Estévez M, López-Periago E, Martínez-Carballo E, et al. (2008) The mobility and degradation of pesticides in soils and the pollution of groundwater resources. *Agr Ecosyst Environ* 123: 247-260.
50. Puglisi E, Cappa F, Fragoulis G, et al. (2007) Bioavailability and degradation of phenanthrene in compost amended soils. *Chemosphere* 67: 548-556.
51. Reid BJ, Jones KC, Semple KT (2000) Bioavailability of persistent organic pollutants in soils and sediments—a perspective on mechanisms, consequences and assessment. *Environ Pollut* 108: 103-112.
52. Wallace KB (1973) Structural behaviour of residual soils of the continually wet Highlands of Papua New Guinea. *Geotechnique* 23: 203-218.
53. Fieldes M (1966) The nature of allophane in soils., Part 1, Significance of structural randomness in pedogenesis. *New Zeal J Sci* 9: 599-607.
54. Wada K (1985) The distinctive properties of Andosol. *Adv Soil Sci* 2: 173-229.
55. Lindner GG, Nakazawa H, Hayashi S (1998) Hollow nanospheres, allophanes ‘All-organic’ synthesis and characterization. *Micropor Mesopor Mat* 21: 381-386.
56. Wells N, Theng BKG (1985) Factors affecting the flow behavior of soil allophane suspensions under low shear rates. *J Colloid Interf Sci* 104: 398-408.
57. Calabi-Floody M, Bendall JS, Jara AA, et al. (2011) Nanoclays from an Andisol: Extraction, properties and carbon stabilization. *Geoderma* 161: 159-167.
58. Garrido-Ramirez EG, Sivaiah MV, Barrault J, et al. (2012) Catalytic wet peroxide oxidation of phenol over iron or copper oxide-supported allophane clay materials: Influence of catalyst SiO<sub>2</sub>/Al<sub>2</sub>O<sub>3</sub> ratio. *Micropor Mesopor Mat* 162: 189-198.
59. Woignier T, Pochet G, Doumenc H, et al. (2007) Allophane: a natural gel in volcanic soils with interesting environmental properties. *J Sol-Gel Sci Techn* 41: 25-30.
60. Adachi Y, Karube J (1999) Application of a scaling law to the analysis of allophane aggregates. *Colloid Surface A* 151: 43-47.
61. Chevallier T, Woignier T, Toucet J, et al. (2008) Fractal structure in natural gels: effect on carbon sequestration in volcanic soils. *J Sol-Gel Sci Techn* 48: 231-238.
62. Chevallier T, Woignier T, Toucet J, et al. (2010) Organic carbon stabilization in the fractal pore structure of Andosols. *Geoderma* 159: 182 - 188.
63. Ghanbarian-Alavijeh B, Millán H, Huang G (2011) A review of fractal, prefractal and pore-solid-fractal models for parameterizing the soil water retention curve. *Can J Soil Sci* 91: 1-14.
64. Bird NRA, Bartoli F, Dexter AR (1996) Water retention models for fractal soil structures. *Eur J Soil Sci* 47: 1-6.
65. Woignier T, Primera J, Hashmy A (2006) Application of the DLCA model to natural gels : the allophanic soils. *J Sol-Gel Sci Techn* 40: 201-207.

66. Primera J, Woignier T, Hasmy A (2005) Pore Structure Simulation of Gels with a Binary Monomer Size Distribution. *J Sol-Gel Sci Techn* 34: 273-280.
67. Meakin P (1983) Formation of Fractal Clusters and Networks by Irreversible Diffusion-Limited Aggregation. *Phys Rev Lett* 51: 1119-1122.
68. Kolb M, Botet R, Jullien R (1983) Scaling of Kinetically Growing Clusters. *Physical Review Letters* 51: 1123-1126.
69. Jullien R, Botet R (1987) Aggregation and Fractal Aggregates: World Scientific.
70. Evans JW (1993) Random and cooperative sequential adsorption. *Rev Mod Phys* 65: 1281-1329.
71. Primera J, Hasmy A, Woignier T (2003) Numerical Study of Pore Sizes Distribution in Gels. *J Sol-Gel Sci Techn* 26: 671-675.
72. Biielders CL, De Backer LW, Delvaux B (1990) Particle Density of Volcanic Soils as Measured with a Gas Pycnometer. *Soil Sci Soc Am J* 54: 822-826.
73. Woignier T, Braudeau E, Doumenc H, et al. (2005) Supercritical Drying Applied to Natural "Gels": Allophanic Soils. *J Sol-Gel Sci Techn* 36: 61-68.
74. Carman PC (1937) Fluid flow through granular beds. *Transactions-ICHEME* 15: 150-166.
75. Woignier T, Primera J, M. L, et al. (2005) The use of silica aerogels as host matrices for chemical species. Different ways to control the permeability and the mechanical properties. *J Non-Cryst Solids* 350: 298-306.
76. Dullien FAL, Brenner H (1979) Porous Media: Fluid Transport and Pore Structure: Academic press. 396 p.
77. Wyllie MRJ, Spangler MB (1952) Application of Electrical Resistivity Measurements to Problem of Fluid Flow in Porous Media. *AAPG Bull* 36: 359-403.
78. Stanley HE, Family F, Gould H (1985) Kinetics of aggregation and gelation. *J Polym Sci Polym Symp* 73: 19-37.
79. Courtens E, Pelous J, Phalippou J, et al. (1987) Brillouin-scattering measurements of phonon-fracton crossover in silica aerogels. *Phys Rev Lett* 58: 128-131.
80. Vacher R, Courtens E, Coddens G, et al. (1990) Crossovers in the density of states of fractal silica aerogels. *Phys Rev Lett* 65: 1008-1011.
81. Herrmann HJ, Stanley HE (1988) The fractal dimension of the minimum path in two- and three-dimensional percolation. *J Phys A-Math Gen* 21: L829.
82. Meakin P, Majid I, Havlin S, et al. (1984) Topological properties of diffusion limited aggregation and cluster-cluster aggregation. *J Phys A-Math Gen* 17: L975.
83. Ramanujan S, Pluen A, McKee TD, et al. (2002) Diffusion and Convection in Collagen Gels: Implications for Transport in the Tumor Interstitium. *Biophys J* 83: 1650-1660.
84. Anez L, Calas-Etienne S, Primera J, et al. (2014) Gas and liquid permeability in nano composites gels: Comparison of Knudsen and Klinkenberg correction factors. *Micropor Mesopor Mat* 200: 79-85.
85. Fosmoe A, Hench LL (1992) Gas permeability in porous gel-silica. In: L.L. Hench JKW, editor. *Chemical Processing of Advanced Materials*. New York: John Wiley and Sons Inc. pp. 897-905.
86. Gross J, Scherer G (1998) Structural Efficiency and Microstructural Modeling of Wet Gels and Aerogels. *J Sol-Gel Sci Techn* 13: 957-960.
87. Reichenauer G, Stumpf C, Fricke J (1995) Characterization of SiO<sub>2</sub>, RF and carbon aerogels by dynamic gas expansion. *J Non-Cryst Solids* 186: 334-341.
88. Dorel M, Roger-Estrade J, Manichon H, et al. (2000) Porosity and soil water properties of Caribbean volcanic ash soils. *Soil Use Manage* 16: 133-140.



- 
89. Fernandez-Bayo JD, Saison C, Voltz M, et al (2013). Chlordecone fate and mineralisation in a tropical soil (andosol) microcosm under aerobic conditions. *Sci Total Environ* 463-464: 395-403.



AIMS Press

© 2015 Thierry Woignier, et al., licensee AIMS Press. This is an open access article distributed under the terms of the Creative Commons Attribution License (<http://creativecommons.org/licenses/by/4.0>)